Global Ecology and Biogeography, (Global Ecol. Biogeogr.) (2010) **19**, 72–84

A Journal of Macroecology

Global Ecology and Biogeography

RESEARCH PAPER

The variation of apparent crown size and canopy heterogeneity across lowland Amazonian forests

Nicolas Barbier[1,3]*, Pierre Couteron[2], Christophe Proisy[2], Yadvinder Malhi[3] and Jean-Philippe Gastellu-Etchegorry[4]

[1]*FNRS-FWA, Laboratoire de Complexité et Dynamique des Systèmes Tropicaux, Université Libre de Bruxelles, 50 Av. FD Roosevelt, CP 169, B-1050 Bruxelles, Belgium,* [2]*IRD-UMR Botanique et Bioinformatique de l'Architecture des Plantes (AMAP), Boulevard de la Lironde, TA A-51/PS2, 34398 Montpellier Cedex 05, France,* [3]*Environmental Change Institute, School of Geography and the Environment, University of Oxford, Oxford OX1 3QY, UK,* [4]*Centre d'Etudes Spatiales de la Biosphère (CESBIO). Université de Toulouse, UPS, CNRS, CNES, IRD, 18 Av. Ed. Belin, 31401 Toulouse, France*

*Correspondence: Nicolas Barbier, FNRS-FWA, Laboratoire de Complexité et Dynamique des Systèmes Tropicaux, Université Libre de Bruxelles, 50 Av. FD Roosevelt, CP 169, B-1050 Bruxelles, Belgium.
E-mail: nbarbier@ulb.ac.be

ABSTRACT

Aim The size structure of a forest canopy is an important descriptor of the forest environment that may yield information on forest biomass and ecology. However, its variability at regional scales is poorly described or understood because of the still prohibitive cost of very high-resolution imagery as well as the lack of an appropriate methodology. We here employ a novel approach to describe and map the canopy structure of tropical forests.

Location Amazonia.

Methods We apply Fourier transform textural ordination (FOTO) techniques to subsamples of very high-resolution satellite imagery freely available through virtual globe software (e.g. Google Earth®) to determine two key structural variables: apparent mean crown size and heterogeneity in crown size. A similar approach is used with artificial forest canopy images generated by the light interaction model (discrete anisotropic radiative transfer, DART) using three-dimensional stand models. The effects of sun and viewing angles are explored on both model and real data.

Results It is shown that in the case of canopies dominated by a modal size class our approach can predict mean canopy size to an accuracy of 5%. In Amazonia, we could evidence a clear macrostructure, despite considerable local variability. Apparent crown size indeed consistently increases from about 14 m in wet north-west Amazonia to more than 17 m for areas of intermediate dry season length (1–3 months) in south and east Amazonia, before decreasing again towards the ecotone with the Cerrado savanna biome. This general trend reflects the known variation of other forest physiognomic properties (height) reported for South America and Africa. Some regions show significantly greater canopy heterogeneity, a feature that may be related to substratum, perturbation rate and/or forest turnover rate.

Main conclusions Our results demonstrate the feasibility and interest of large-scale assessment of rain forest canopy structure.

Keywords
Forest structure, Fourier transform textural ordination, rain forest, remote sensing, South America.

INTRODUCTION

Tropical forests are a major component of the carbon cycle, and important efforts are being made to quantify their spatial and temporal dynamics in a context of rapidly changing environmental and human pressures (Malhi & Phillips, 2005; Wright, 2005). In particular, the international decision to reduce carbon emissions linked not only to deforestation but also to forest *degradation* (reducing emissions from deforestation and degradation (REDD), **United Nations Framework Convention on Climate Change** conference, Bali, December 2007) has necessitated the development of reliable operational methods to

DOI: 10.1111/j.1466-8238.2009.00493.x

monitor forest structure at regional to continental scales (Defries *et al.*, 2007). This recent renewed impetus has led to a surge of interest in mapping the structure and biomass of tropical forest regions.

One approach to obtaining such information is through spatially extensive field inventories. Whilst providing important information on forest structure (typically diameter distributions) and allometry, these approaches can be limited by their spatial coverage and the difficulty of accessing many remote tropical forest regions. Useful complementary information on canopy and crown structure can be obtained from remote sensing approaches. Airborne remote sensing data (e.g. Lidar (Véga & St-Onge, 2008) and canopy video stereography) are potentially very powerful but are expensive to acquire and present challenging data management issues. Satellite remote sensing (whether optical or radar band L) provides useful insights into structure and phenology but is usually limited by low spatial resolution. These data are generally used without reference to texture, on a pixel-wise basis (but see Weishampel *et al.*, 2001; Saatchi *et al.*, 2007). Moreover, these signals have been shown to saturate for intermediate biomass (*c.* 250 t ha^{-1} Mougin *et al.*, 1999; Foody, 2003) or leaf area index (LAI) values (Huete *et al.*, 2002), preventing their application in the investigation of structure change in natural pluri-strata forests for which biomass can frequently reach 500 t ha^{-1}. Attempts to produce non-saturating vegetation indices (e.g. an enhanced vegetation index) with MODIS data exist, but the results obtained, for instance concerning the temporal variation of the indices, remain difficult to interpret (Huete *et al.*, 2006; Myneni *et al.*, 2007; Saleska *et al.*, 2007).

Very high-resolution (VHR) data, i.e. of approximately 1-m resolution, are now becoming widely available from commercial satellites (Ikonos, QuickBird, Spot5). However, exploiting the thematic information conveyed by these images requires taking their geometrical/textural characteristics into account more than the individual pixel values. Very encouraging attempts have been published recently to characterize the textural properties of VHR canopy images, on the basis of spatial autocorrelation methods such as variography (Bruniquel-Pinel & Gastellu-Etchegorry, 1998), lacunarity analysis (Frazer *et al.*, 2005; Malhi & Roman-Cuesta, 2008) and two-dimensional power spectral analysis (Fourier transform) (Couteron *et al.*, 2005; Proisy *et al.*, 2007). As the dimensionality of the resulting multiscale indices is inherently high, multivariate ordination methods (e.g. principal components analysis, PCA) are required to characterize and compare forest textural properties over large areas and many images (Couteron *et al.*, 2005; Frazer *et al.*, 2005). Attempts have also been made to detect and map individual tree crowns, either manually or automatically, but validation proved to be challenging (Asner *et al.*, 2002; Palace *et al.*, 2008).

Another limitation to the use of VHR data has been the expense involved in acquiring targeted data from commercial providers. However, many of these images are now freely available from providers such as Google Earth®, albeit in a form that prevents detailed analysis of pixel-by-pixel data. Nonetheless, these freely available images do provide sufficient information to derive textural properties.

In this paper we present a novel application of freely available Google Earth® data to map canopy structure and heterogeneity across the Amazonian forest biome. The analysis is based on Fourier transform textural ordination (FOTO), which produces an ordination of the canopies in function of the length scale (spatial frequency) distribution and dominance. In other words, canopies are sorted as a function of the presence of one or several modal apparent crown sizes. In this contribution we shall thus refer to the value of the dominant apparent crown size (ACS) as well as to its degree of dominance (homogeneity). Our aims are to:

1. Evaluate the variation in apparent crown size in forest canopies across the region.

2. Evaluate the variation in homogeneity in forest canopies across the region.

3. Assess the impacts of sun-angle and systematic biases in image acquisition on determination of these canopy parameters, using both artificial canopies obtained using a light interaction model (discrete anisotropic radiative transfer, DART; Gastellu-Etchegorry *et al.*, 1996) and an analysis of real forest canopy data.

4. Interpret these findings in the context of what is known about Amazonian forest ecology and geomorphology.

METHODS

Sampling and imagery

The study region corresponds to the extent of Amazon forests *sensu lato*, i.e. the continuous stretch of forest covering the Amazon and Orinoco watersheds and the Guyana Shield (Eva *et al.*, 2004). We concentrate on lowland *terra firme* forests, using forest cover masks derived from the maps of Saatchi *et al.* (2007) and Eva *et al.* (2004). We therefore included dense forests, open forests, bamboo forests, liana/dry forests and seasonal forests as a single entity, but excluded both seasonally flooded and montane forests types.

Two hundred sample areas (1 km^2) were identified in Google Earth®, within homogeneous, apparently undisturbed, closed canopy lowland terra firme forests on relatively flat ground, where VHR DigitalGlobe QuickBird images were available. These images consist of true colour composites of the blue (450–520 nm), green (520–600 nm) and red (630–690 nm) bands, sharpened to 0.6-m resolution using the panchromatic band. The images are orthorectified. We could not find information on possible radiometric corrections. Image extracts were exported from the Google Earth Pro® interface at the nominal resolution of the QuickBird imagery (0.6–0.7 m). For comparability with model simulations (see below), images were then resampled (averaging aggregation) to 2-m pixel resolution and converted to greyscale levels.

Metadata for the QuickBird imagery used in this study are listed in Table S1 in Supporting Information. Figure 6 (later in the results section) presents the spatial variation and frequency

distributions of the acquisition parameters. Sun vertical angle (θ_s) varied between 44.4° and 73.5° (0° towards horizon), view zenith angle (θ_v) between 1° and 21° and relative sun–sensor angle (φ_{s-v}) between 0.0° (backscattering, i.e. the sun is located behind the sensor) and 178.2° (forward scattering).

The FOTO method

The use of the FOTO method to characterize the spatial structure of vegetation in VHR imagery has been presented elsewhere (Couteron, 2002; Couteron *et al.*, 2005, 2006; Proisy *et al.*, 2007). In brief (Fig. 1), vertical aerial canopy images of adequate size (see below) were either extracted from satellite imagery or provided by DART simulations, and subjected to a two-dimensional Fourier transform [via the fast Fourier transform algorithm; implemented in Matlab® (MathWorks, Inc.)], and to subsequent computation of the two-dimensional periodogram or power spectrum, i.e. the squared amplitude of the Fourier transform. The latter expresses the apportioning of the image variance (or power) into frequency bins along the two Cartesian axes, or equivalently, for different spatial frequencies and orientations in polar axes. This characterization of images in terms of spatial frequencies constitutes a very efficient way to quantify pattern scale and intensity, especially but not exclusively (Couteron *et al.*, 2006) for repetitive patterns or textures, such as those formed by forest canopies. As we were not interested here in anisotropic properties of the images, periodograms were simplified through the computation of the radial spectra (r-spectrum) that is the average of the frequency information across azimuthal directions of space. Frequencies are expressed in cycles hm^{-1}, that is the number of repetitions over a 100 m distance.

The size of sampling unit windows (i.e. image extracts) was chosen to include several repetitions of the largest pattern of interest. In the present case, average tree crown diameters are not expected to exceed 30 m, and window size was therefore set to 150 m (at least five repetitions). Substantial variations (by a factor of three or more) of the window size have, however, been shown to provide equivalent results in terms of texture gradients (Couteron *et al.*, 2006; Proisy *et al.*, 2007).

A table was constructed (Fig. 1) containing the r-spectra of all analysed unit windows. In this table columns correspond to the set of Fourier harmonic spatial frequencies and rows to individual windows. The table was centred and standardized across lines (i.e. column-wise subtraction of the mean and division by the standard deviation) and an ordination performed (PCA) to identify the main gradients of variation between windows on the basis of their spatial (frequency) attributes. In order to attenuate the variability resulting from varying acquisition parameters of the QuickBird scenes, a variant (Fig. 1) of this ordination method was used, in which unit windows were separated into pre-defined bins of similar acquisition parameters. Standardization was then performed separately for each bin, and the resulting standardized spectra were reunited again in a single table for ordination (hence the name partitioned standardization). The objective of this approach was to minimize the variability component due to instrumental discrepancies. This is efficient only if the complete observable canopy texture gradient is present in each of the instrumental bins.

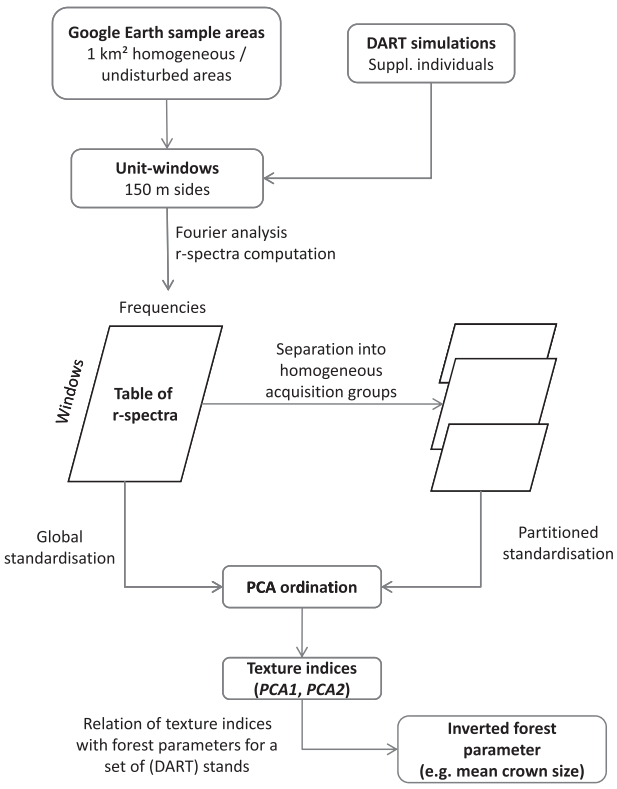

Figure 1 Flow chart illustrating how Fourier transform textural ordination (FOTO) analysis is applied in this paper on both real-world (QuickBird) and simulated (discrete anisotropic radiative transfer, DART) images with either 'global' or 'partitioned' standardization of r-spectra.

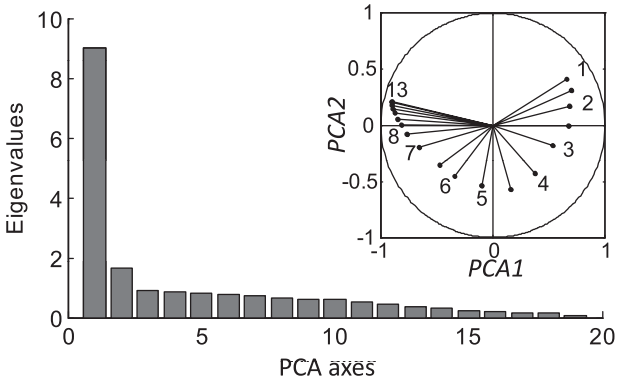

Figure 2 Principal components analysis (PCA) of satellite imagery data (QuickBird). Plot of eigenvalues. Inset: correlation of the original variables, i.e. the frequencies of the Fourier r-spectra, expressed in cycles hm^{-1}, with the PCA axes. Some intermediate values are not labelled for clarity.

Simulating reflectance images of forest canopy

A set of artificially generated forest canopy scenes was simulated using DART (v. 2.0.4, CESBIO) in order: to (1) verify the relationship between the textural ordination and controlled morphological parameters – in particular crown diameters, and (2) quantify the impact of varying acquisition parameters on the results of the FOTO analysis. A detailed description of the model has been presented elsewhere (Gastellu-Etchegorry *et al.*, 1996; Bruniquel-Pinel & Gastellu-Etchegorry, 1998), and we will limit ourselves to a quick overview. A DART scene is modelled as a three-dimensional array of volumetric cells (or voxels), each of which presents specific optical properties (transmittance and phase functions) depending on the cell type (soil, water, trunk, leaves, etc.). Certain voxels (e.g. leaves) are modelled as turbid media with volume interaction properties and others (trunks, soil) as solid media with surface properties. Structural characteristics within the cell (e.g. LAI or leaf angle distribution) influence the cell's optical properties. Radiation transport (i.e. the scattering of rays from each cell) is simulated iteratively in a discrete number of directions. Interaction with the atmosphere or soil topographic features can possibly be added, as well as wavelength-specific behaviours. However, in the present study, we kept to a monospectral (visible) domain on a flat terrain without atmospheric effects. DART scenes were modelled using the same extent and resolution as the satellite unit windows (150 m and 2 m, respectively).

Trees were modelled using an ellipsoidal approximation of the crowns, with trunks randomly located within a given distance (l, location radius; Table 1) from the nodes of a square mesh (internode distance r). Only two strata were included, with distinct normal distributions (i.e. distinct mean and standard deviations) of the morphological parameters. Table 1 shows the ranges of values for the morphological parameters used to model the dominant stratum, as well as the allometric relationships linking these parameters. These relationships were derived from a set of 54 Bolivian moist-forest species (Poorter *et al.*, 2006), although we took a simpler, linear relation between diameter at breast height (DBH) and height (H), instead of the asymptotic equation given by the authors. Indeed, the latter could not be used for realistic extrapolations above the maximal values studied by the authors, that is a DBH_{max} of *c.* 1.6 m (asymptotic H_{max} = 45 m). In our simulations, mean crown diameters of the dominant stratum ranged between 5 and 25 m. Acquisition parameters (viewing zenith angle, sun vertical angle and sun-sensor horizontal angle) were also made to vary independently from each other and from the morphological parameters (Table 1), within a similar range of variation as that observed in the set of actual (QuickBird) images (Table S1 and Fig. 6). A total of 330 scenes were thus modelled.

RESULTS

Ordination results and crown size inversion

The ordination of the 7200 (200 areas × 36 unit windows/area) satellite views of Amazonian canopies synthesized most textural information along the two first PCA axes. The first axis accounted for 47.6% of the variation in image spatial structure (Fig. 2), while the second axis only contributed 8.7%. As with previous applications of the FOTO methods to tropical forest canopies (Couteron *et al.*, 2005; Proisy *et al.*, 2007), the correlation circle (Fig. 2, inset) showed a typical clockwise distribution of the frequencies (expressed in cycles hm^{-1}, i.e. the number of repetitions of the template periodic pattern on a 100-m reference distance). In other words, the gradient along PCA1 ranges from windows characterized by small frequencies (2–3 cycles hm^{-1}, thus a wavelength between 50 and 30 m) up to those characterized by large frequencies (8–10 cycles hm^{-1}, wavelength between 12.5 and 10 m), while negative PCA2 values reflect the relative prominence of intermediate frequencies around 5 cycles/hm (wavelength of about 20 m), therefore allowing a finer characterization of medium-scale textures. Hence the position along the PCA1 axis indicates the mean length scale of image spatial structure, whereas radial distance from the PCA origin indicates relative dominance by a single length scale, i.e. homogeneity of the image spatial structure. A selection of character-

Table 1 Parameter values and allometry rules used to generate artificial stands and to run the DART light interaction model.

Parameter symbol	Definition	Range or allometry rule	Std. dev.	Unit
r	Mesh size	5–25 (10 levels)	d/4 (on location)	m
l	radius of tree positions around nodes	r/2		
d	Crown diameter (ellipsoid horizontal axes)	r	d/4	m
A	Crown area (intermediate parameter)	$0.25\pi d^2$		m^2
H	Total height (intermediate parameter)	$\exp[(\ln A + 1.853)/1.888]$		m
h_c	Crown height	$\exp(-1.169 + 1.098 \ln H)$	h_c/4	m
h_t	Trunk height below crown	$H - h_c$	h_t/4	m
DBH	Trunk diameter below crown	H/42	DBH/4	m
θ_s	Sun vertical angle	45–75 (three levels)		Degrees from horizon
θ_v	Sensor zenith angle	0–24 (three levels)		Degrees from zenith
φ_{s-v}	Difference between sun and sensor azimuth angles	0–180 (three to four levels)		Degrees

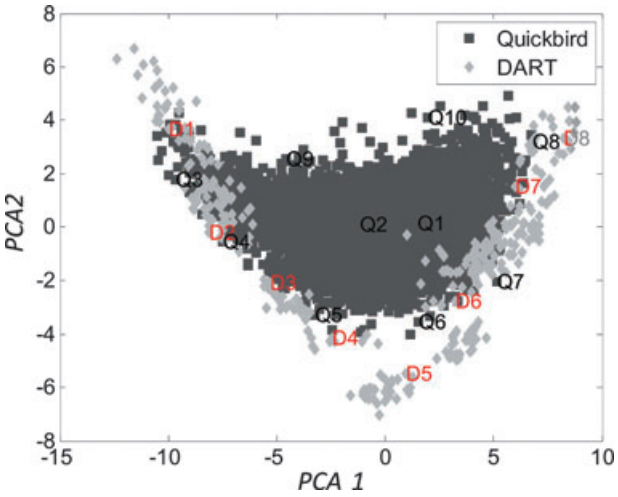

Figure 3 Principal components (PCA) plot of QuickBird (satellite) unit-windows with discrete anisotropic radiative transfer (DART) (simulated) windows added as supplementary individuals. Each point corresponds to a single 150-m side unit window, characterized by its Fourier r-spectrum. Only homogeneous (marginal) textures are produced by the DART model, i.e. textures dominated by a single spatial frequency. QuickBird (Q1–Q10) and DART (D1–D8) unit windows characterizing the gradient of homogeneous canopies as well as typical heterogeneous canopies, as shown in Fig. 4 and in Figs S1 & S2, are localized in the PCA plane.

istic windows (provided in the Supporting Information) illustrates the overall gradient of observed canopy textures (Figs S1 & S2) and of their r-spectra (Fig. S3). The position of these windows in the PCA is presented in Fig. 3.

To help interpret the relationship between the results of textural ordination and forest morphological parameters, the position of DART-simulated images in the ordination is also shown (Fig. 3). Although modelled stand structures were very simple, forest canopy mock-ups are visually realistic (Fig. 4) and the limits of the two clouds closely match in the PCA plane (Fig. 4), although DART stands only occupy the cloud's margins. The latter result confirms that points located away from the PCA origin correspond to more homogeneous canopies, which are dominated by a single spatial scale.

Quadratic regressions between the two first PCA axes and mean crown size (d) of the DART unit windows showed the potential of the method for retrieving crown size values in real-world stands. R^2 values reached 0.96 for the following model: $d = 16.553 + 0.904\ \mathrm{PCA1} - 0.019\ \mathrm{PCA1}^2 + 0.619\ \mathrm{PCA2} - 0.018\ \mathrm{PCA2}^2$. This result was obtained without any correction linked to the variation of the acquisition parameters (as will be implemented below). Figure 5 presents the relation between inverted mean crown sizes (on the basis of the quadratic model) and mean crown sizes (d) used for DART modelling. A simpler linear fit with PC1 scored an R^2 of 0.88: $d = 15.206 + 0.871$ PCA1.

Both these models (quadratic and linear) were used in subsequent analyses to infer ACS in real-world (QuickBird) images. The adjective 'apparent' aims here at underlining the possibility that a dominant scale in 'complex' real-world canopies, as opposed to our DART scenes, might in some cases correspond to a modal size of crown clumps rather than individual tree crowns.

Influence of interscene variation of acquisition parameters

The very high correlation obtained for DART scenes between textural ordination results and crown diameters in the absence of any correction for varying acquisition angles (see previous section) suggests that the influence of acquisition parameters could also be small for our set of real-world images. However, the geographical variation of the sun vertical acquisition angle, θ_s, presents a strongly organized spatial pattern (Fig. 6a), in which relatively low sun vertical angles are more abundant in the southern tip of the study area. This is because most cloud-free image acquisitions occur in the dry season. In southern Amazonia this corresponds to the period May–September, when the sun (and hence the tropical convection zones) is above the Northern Hemisphere and sun angles are hence low. In northern Amazonia (near the equator) the correlation between sun angle and cloud-free conditions is less strong. The variation of θ_v and φ_{s-v} does not show any clear spatial pattern over the study area (Fig. 6b,c).

Therefore, it was necessary to investigate, and if necessary mitigate, potential bias due to the non-random geographic distribution of the sun vertical acquisition angle. A first qualitative indication of the limited importance of bias is that the pattern of geographical variation of θ_s is quite different from the one found for canopy texture, as it is shifted towards the south and does not present the same features towards the Guiana Shield. However, linear regression of PCA1 values with θ_s gave a significant result ($P < 0.001$) (Fig. 7a). No significant influence of the two other angles could be evidenced (figures not shown). Performing a partitioned standardization prior to ordination, i.e. standardizing r-spectra within bins of homogeneous acquisition angles, allowed us to factor out unwanted influences of acquisition conditions on the quantification of the canopy textural gradient. Partitioned standardization of QuickBird unit windows in as few as three levels of θ_s indeed allowed the removal of all significant trends (Fig. 7b) due to this factor. Results presented hereafter are thus produced using PCA values computed using the latter partitioning approach.

We also checked for possible interactions between acquisition angles and the crown size–texture relationship using the simulated images. For instance, extended shadows due to lower solar angles could have a more important effect on the characterization of forests made of larger trees. Using a linear model, we first checked for the homogeneity of slopes between crown diameter and PCA1, with the different levels (experimentally defined, Table 1) of acquisition angles taken as a discrete factor. This allowed us to discard the existence of any significant interaction between the crown size–texture relationship and acquisition angles. However, the ANCOVA indicated a significant

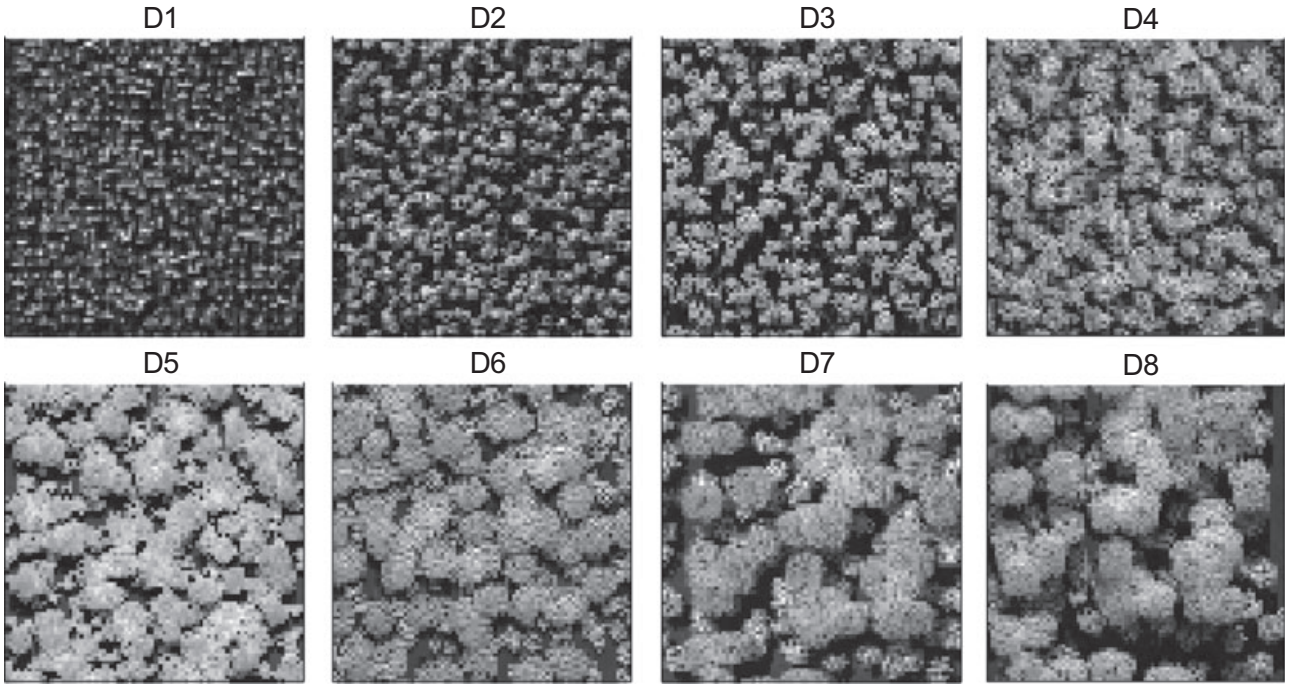

Figure 4 Discrete anisotropic radiative transfer (DART) simulated unit windows characterizing the gradient of mean crown size. These modelled canopy images are produced using the DART light transfer model on three-dimensional artificial stands corresponding to the parameter range summarized in Table 1. See Fig. 3 for localization of these windows in the first principal components analysis plan.

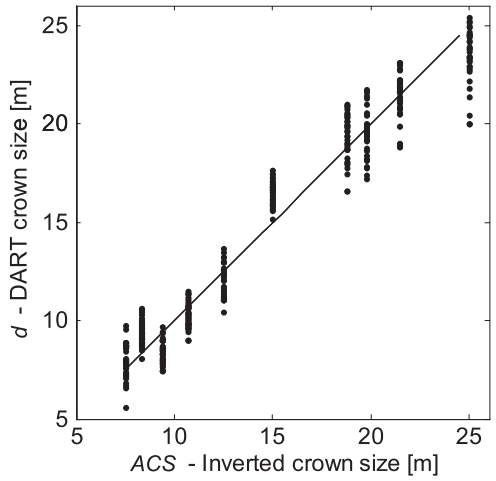

Figure 5 Match between predicted (inverted) apparent crown size (ACS), obtained using a quadratic model involving PCA1 and PCA2, and the 'actual' mean crown diameter (d) of the discrete anisotropic radiative transfer (DART) simulated scenes. The 1:1 line is also represented. The r^2 of the linear fit is of 0.95 and exactly matches the 1:1 line.

($P < 0.05$) effect for θ_v and φ_{s-v}, and a very significant effect for θ_s ($P < 10^{-5}$) on PCA1 values. No significant interaction between the different angles could be evidenced. Therefore, acquisition properties, and in particular sun vertical angle, did have a small influence on the textural ordination of DART unit windows. Here again, the partitioned standardization procedure allowed efficient minimization of the influence of acquisition angles.

Mapping apparent crown size in Amazonia

We have shown above that PCA coordinates could be used to infer mean crown sizes, or in the case of real, potentially complex canopies, ACS. We first used the simple linear model based on PCA1 values (see above), to derive the apparent crown size of the 7200 QuickBird unit windows. These ACSs were then averaged for each sample area, to provide a sample of 200 points with mean ACS values. The symbols in Fig. 8(a) show the spatial distribution of these mean ACS values across Amazonian *terra firme* forests. In the same figure, the colour scale represents a kriged interpolation (ordinary kriging, spherical model; Cressie, 1993) of ACS for terra firme forests. Hatched and cross-hatched areas represent zones where the kriging standard error is above 1.95 m and 2 m, respectively. Interpolation error is higher in areas where sampling is relatively sparse, such as French Guyana, southern Colombia or north-eastern Brazil.

Figure S4 shows a second ACS map, resulting from a more restrictive approach based on the quadratic inversion model involving PCA1 and PCA2, but with inference limited only to the most homogeneous unit windows. For this map we took only the subset of unit windows located beyond the 75% quantile of the distance to the centre of the PCA. These are image

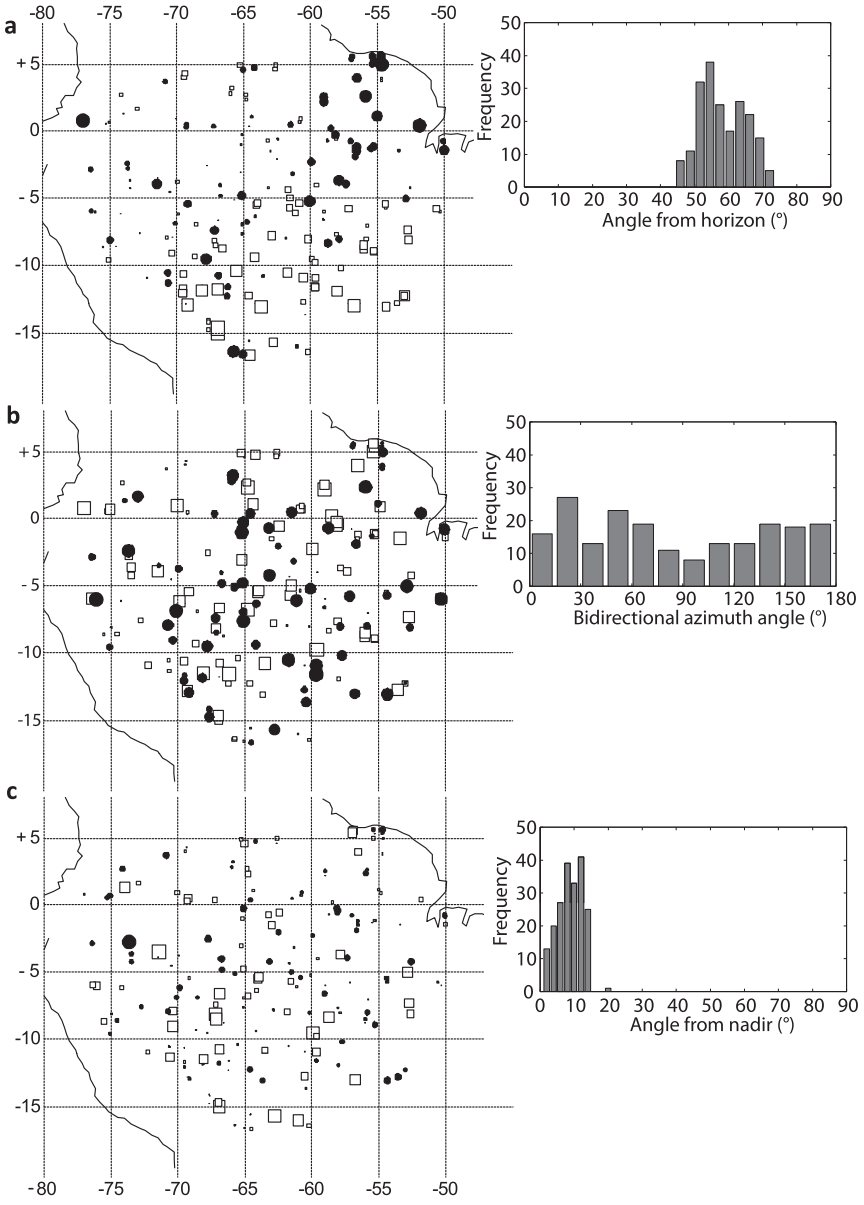

Figure 6 Distribution of acquisition angles of the QuickBird set of images with maps of parameter values over the study area (left) and histograms of absolute frequencies (number of images). (a) Sun vertical angle, θ_s. (b) Sun–sensor azimuth angle, φ_{s-v}. (c) View zenith angle, θ_v. Symbols represent locations of sampled satellite (QuickBird) images. Symbol size is proportional to the standardized value of each parameter. Squares represent negative standardized values, circles represent positive ones. Geographical coordinates; datum, WGS 84.

types where the relationship between image length, scale and crown size has been validated by our modelling with DART above. The gain in confidence in local ACS values is balanced by an increase in kriging standard error (above 3 m) induced by a reduced sample ($n = 145$).

A similar large-scale pattern of the variation in ACS across Amazonian terra firme forests was present in both maps (Figs 8a & S4). ACSs tend to be highest (> 16 m) in a broad east–west band stretching 5–10° S of the equator, and also fairly high (> 15 m) in the contiguous region in north-eastern Amazonia. Small crown sizes (< 14 m) dominate in north-western Amazonia (although image density is lower because of cloudier conditions) and also at the very southern fringe. Hence broadly there is a directional gradient in ACS, with the lowest values in the north-west and higher values to the south, south-east and east, although there is substantial local variability in ACS probably related to local landscape and hydrological conditions. The overall pattern of variation in canopy texture proved robust with regard to alternative interpolation procedures (i.e. different kriging models or inverse distance weighting) or to the facultative correction of acquisition parameters.

Mapping canopy homogeneity in Amazonia

Another interesting textural characteristic of the canopy is its degree of homogeneity (i.e. single scale dominance). We therefore investigated the spatial distribution of scale-specific (peak dominated) versus multiscale canopies (flat spectrum) in Amazonian terra firme forest. The index used was the standardized distance to the PCA origin (only for the angular directions in the PCA for which the distance corresponded to single peak dominance, i.e. PCA2 values ≤ 0). The resulting pattern (Fig. 8b) is different from the ACS pattern presented above. There is no clear overall regional trend in canopy homogeneity, but distinct

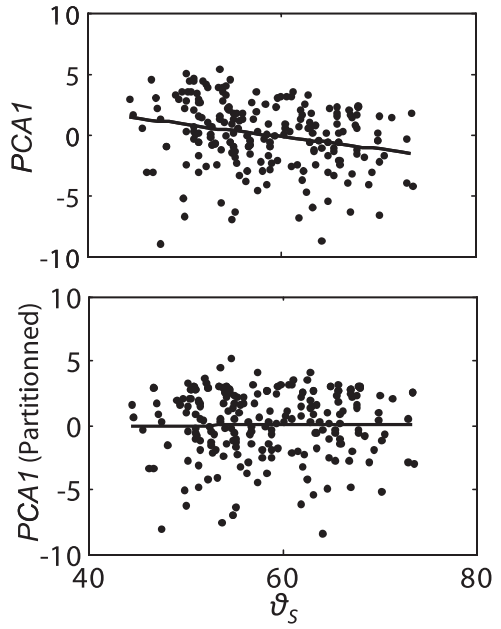

Figure 7 Linear regressions between the PCA1, i.e. the main textural gradient in the image dataset, and sun vertical angle for satellite (QuickBird) images ($n = 200$, $r^2 = 0.07$). Each point corresponds to the average PCA1 values for one sampling zone (i.e. 36 unit windows extracted from a given QuickBird image). (a) After a global, non-partitioned standardization ($r^2 = 0.06$). (b) After a partitioned standardization with three bins of sun vertical angle ($r^2 < 10^{-4}$).

regions dominated by more heterogeneous canopies (square symbols, brownish interpolated values) do stand out. These are in: (1) north-west Amazonia (ranging from Ecuador through northern Peru, southern Colombia and north-western Brazil), (2) northern Bolivia in south-western Amazonia, and (3) north-eastern Amazonia, ranging from the Amazon River to the Guyanas. Zones dominated by homogeneous canopies are less distinct, but there is an indication of such a zone at the eastern fringe of Amazonia, and also perhaps in central-northern Amazonia.

DISCUSSION

The applicability of the FOTO method

In this paper we have shown the potential of the FOTO method to consistently provide non-saturating, large-scale estimates of canopy structural properties observed in VHR imagery, particularly imagery now freely available on virtual globe software.

An important advantage of FOTO as performed here lies in its relative independence from the absolute value of both mean and variance of the images, since the mean-centred images are characterized in terms of the proportion of their variance (however large it is) explained by the spatial frequency bins (Diggle, 1989; Mugglestone & Renshaw, 1998). Variations in contrast and luminosity, or poor radiometric alignments between images, do not therefore have much influence on the result of the analysis, as long as the spatial arrangement of relative greyscale values is conserved. This is of course an important pre-requisite for the use of virtual globe imagery, or for tropical applications in general, for which the user does not have access to base (i.e. multispectral and atmospheric) data to perform radiometric corrections. However, variations in other scene acquisition parameters, namely sun and sensor vertical angles and sun–sensor azimuthal angle, had the potential to alter the observed size and proportion of the tree shadows, and therefore the very spatial arrangement we aim to characterize. For instance, for the case of VHR images of Amazon rain forests, Asner & Warner (2003) discussed the variation of the shadow fraction in a set of 29 Ikonos® images taken in the LBA dataset. Using their data (Table 2 of Asner & Warner, 2003), we found that the relative sun–sensor azimuth angle explained a significant part ($R^2 = 0.25$, $P < 0.001$) of the mean shadow fraction. However, we could show both on the basis of real world data and through the DART modelling of structurally and radiometrically realistic stands, that the FOTO method is only marginally dependent on sun-viewing geometry, and that an appropriate, simple correction (partitioned standardization) can completely remove this dependence.

Explaining spatial variation in crown size and heterogeneity

Any spatial trend in ACS is likely to be influenced by the rainfall regime and local landscape topography, hydrology, soil type and perhaps other biogeographical quirks. One useful metric of the rainfall regime is the number of months with rainfall below 100 mm (i.e. dry season length, or DSL; Sombroek, 2001), which is plotted in Fig. 9(a). It can be seen that the broad band of larger ACSs corresponds to a region with a significant but moderate dry season (1–3 months), with a maximum ACS (*c.* 17 m on average) at a DSL of 2 months. Regions with no dry season correspond to small crown sizes, as do regions with a long dry season (> 5 months), where elements of savanna (Cerrado) vegetation may begin to appear. Hence maximum ACS shows a unimodal relationship with DSL, but within this broad envelope there can be substantial local variability in ACS. The ecological reason for the relationship between ACS and DSL is not clear: moderate seasonal drought and a clear, sunny dry season may competitively favour a stratum of larger-canopy, deeper-rooted trees, but stronger seasonal drought may cause hydraulic limitations and a restriction in crown size. This very consistent pattern of variation has already been reported through field observations of other structural parameters, such as maximum tree height, and indeed the whole forest physiognomy (Ellenberg, 1975; Longman & Jenik, 1987; Richards, 1995). According to the same authors, the most humid Central African forests also show a decrease in tree height, biomass and diameters. For Amazonia, Saatchi *et al.* (2009) also report that the north-west (most humid) region presents a distinctively lower fraction of large trees.

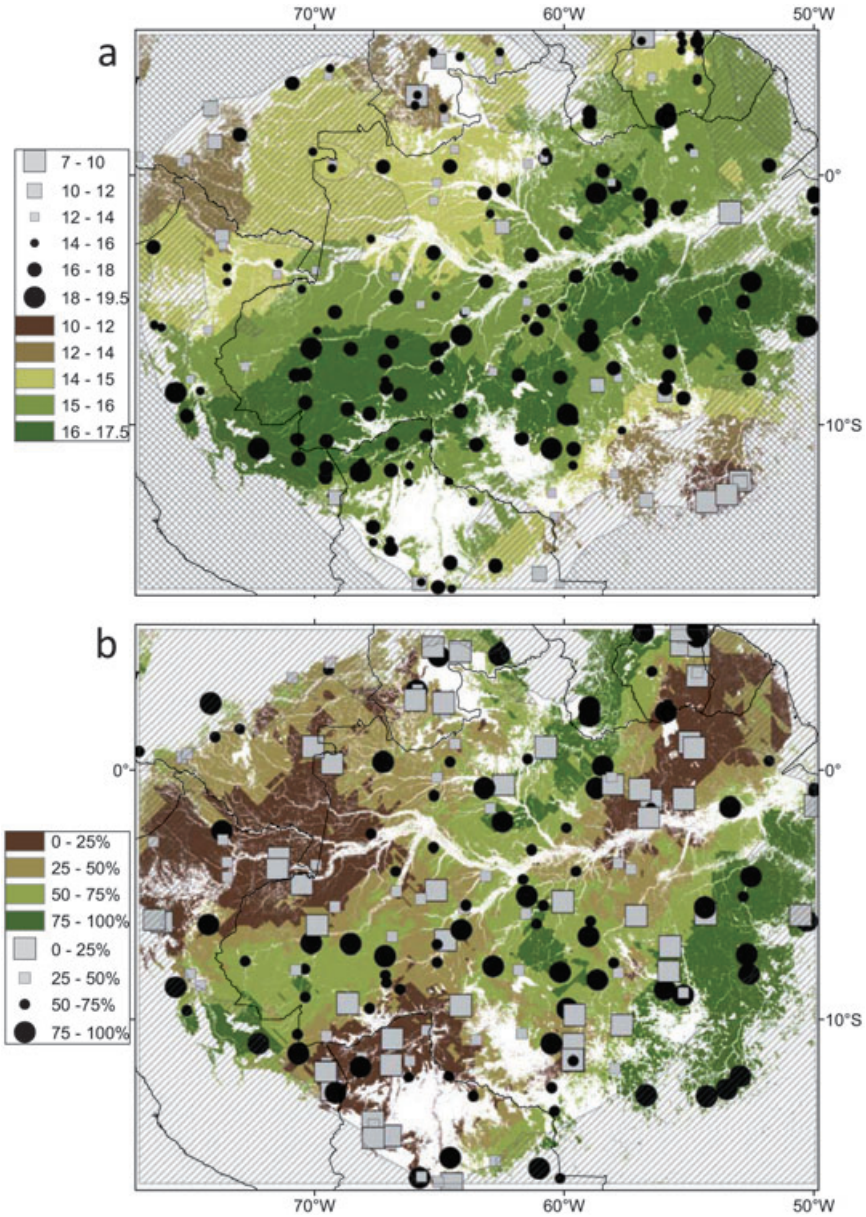

Figure 8 Maps of canopy texture variation in lowland *terra firme* forests (pointwise and interpolated values). (a) Apparent crown size (in m) estimated using a linear function (model inversion) of the first component of the principal components analysis (PCA; $n = 200$). Symbols represent the location of sampled satellite (QuickBird) images. Symbol size is proportional to the deviation from the mean. Squares represent values below the mean, circles represent values above the mean. Hatched zones indicate a kriging standard error above 1.95 m; cross-hatched zones indicate a kriging standard error above 2 m. (b) Quantiles of the distance to PCA origin, quantifying the degree of homogeneity of the canopy (higher values are dominated by a single scale). Symbols represent locations of sampled satellite (QuickBird) images ($n = 200$). Symbol size/shape indicates the distance to PCA origin (in quantiles of the distribution in the corresponding angular sector). Hatched zones indicate a kriging standard error above 20%. In both (a) and (b), PCA is run using a partitioned standardization (three bins of sun vertical angle) of the r-spectra. Interpolation uses ordinary kriging (spherical model). Geographical coordinates; datum, WGS 84.

Soils and land form might be expected to explain some of the regional variability in ACS (Fig. 9b,c). However, the band of large ACS ranges over regions of crystalline shield in the east (dominated by well-drained ferralsols and nitisols), through low, poorly drained Amazonian peneplain in the centre-south (dominated by plinthosols), through to slightly more fertile and hilly landscapes in the south-west (dominated by acrisols and cambisols), with little apparent trend in mean ACS. The region of small ACS in the north-west contains areas of poorly drained, low-elevation, plinthosol-dominated Amazonian peneplain; hence high rainfall and poor drainage and soil structure may interact to favour small crown sizes in this region. Hypotheses

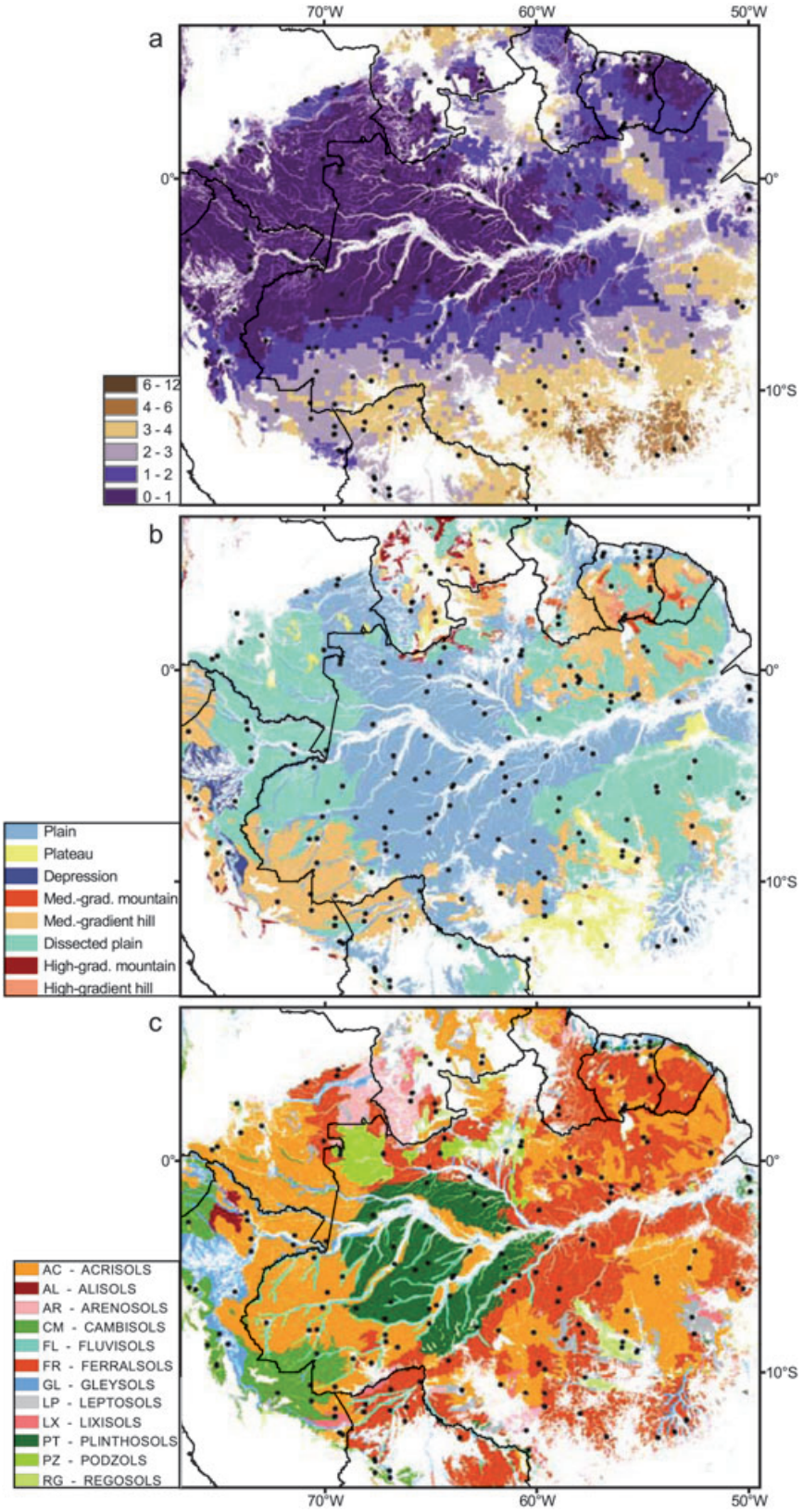

Figure 9 Maps of potential environmental drivers. (a) Dry season length, in months below 100 mm rainfall (source TRMM; Wolff *et al.*, 2005). (b) Land types (source FAO *et al.*, 1998). (c) Dominant soil classes (source FAO *et al.*, 1998). Points represent locations of sampled satellite (QuickBird) images.

proposed by Longman & Jenik (1987) to explain the decrease in tree size towards the high-rainfall region also include higher leaching of nutrients or lower photosynthesis rates due to permanent overcast (cloudy) conditions. The fact that phenological (seasonal) variation in rainforests seems mainly driven by insolation (and not rainfall) (van Schaik *et al.*, 1993; Wright & van Schaik, 1994; Huete *et al.*, 2006; Myneni *et al.*, 2007) suggests some support for the latter hypothesis, meaning that radiation would be a limiting element in this ecosystem. However, there is no evidence for lower forest productivity in the north-western region compared with other parts of Amazonia (Malhi *et al.*, 2004; Aragão *et al.*, 2009), suggesting little limitation of photosynthesis in this region. Moreover, there is no obvious link between forest productivity and tree size: Malhi *et al.* (2004) demonstrated that some of the least productive forests in Amazonia (in eastern Amazonia) had the highest biomass and largest mean tree size.

In contrast to crown size, canopy heterogeneity (computed as the standardized distance to PCA centre) shows no obvious relationship to rainfall regime. However, some distinct regional patterns hint at large scale modulation mechanisms or drivers. In terms of the forest structure, a heterogeneous canopy may reflect: (1) higher rates of mortality of large trees linked to biotic interactions (competition, pathogens) or to soil constraints, or (2) more frequent perturbation events (e.g. windthrows) inducing a mosaic of patches of different ages (Aubréville, 1938; Watt, 1947; Oldeman, 1990), or (3) other unknown, possibly endogenous, community dynamics leading to a canopy characterized by the presence of scattered emergent trees. Relatively higher turnover rates have been evidenced (Phillips *et al.*, 2004) in the area corresponding roughly to the heterogeneous forest patch in the north-west, an area also characterized by a small ACS (see above) and high rainfall. The same factors causing a decrease in trees in the highest rainfall zone size may therefore also trigger faster stand dynamics, conditioning a more heterogeneous canopy. In terms of soils, the area features a mix of relative extremes, from younger, possibly more fertile, soils at the foot of the Andes (cambisols), through deep acrisols to very shallow plinthosols in the peneplain.

In the north-east, by contrast, the high-heterogeneity area corresponds to an area of crystalline shield and adjoining lowlands dominated by ferralsols, and ranging from a fairly strong dry season near the Amazon River to little dry season in the Guyanas. Similarly, the heterogeneous area in the south-west shows no obvious relationship to land form, soil type or rainfall. Both these areas are zones of medium to high ACS, and heterogeneity here may reflect preponderance of large emergent trees (Saatchi *et al.*, 2009). This north-eastern region is also the region most affected by El Niño associated drought (Malhi & Wright, 2004), and there may be a causal relation between the risk of occasional drought and domination by large, possibly deep-rooted trees.

In addition, biogeography may play a role. In the north-east, the large trees often belong to a few distinct families (e.g. Leguminaceae, Lecythidaceae, Chrysobalanaceae). Many of these families (especially legumes) may dominate in this region because of their tendency to have large seeds, a successful reproductive strategy in the poor soils of the north-east (ter Steege *et al.* 2006). They also happen to have several species that form large trees. Hence an unrelated biogeographical factor (lower soil fertility favouring families with large seeds) may have consequences for ACS and canopy heterogeneity (the frequency of emergent trees). Similar, undocumented biogeographical factors may be at play in other regions.

An obvious next step is a more detailed exploration of any relationship between crown size and heterogeneity and forest structural parameters determined from ground surveys such as the RAINFOR network (Malhi *et al.*, 2002, 2006; Baker *et al.*, 2004; Saatchi *et al.*, 2009). These include metrics such as biomass, large tree dominance, basal area, productivity and turnover. Some theories (Enquist, 2002) and field data (Poorter *et al.*, 2006) suggest that general allometric relationships do exist in natural forests that may help us understand why good correlations are found between canopy features (FOTO indices) and field measured stand parameters (Couteron *et al.*, 2005; Proisy *et al.*, 2007). This possibility opens promising research avenues, both for the corpus of ecological theory and for practical applications regarding forest resource monitoring (including biomass and carbon). Any relationship with biomass would be particularly useful in the context of intense current interest in mapping the biomass of tropical forests as a tool for assigning carbon value to intact tropical forests. Our analysis suggests that there may not be any simple relationship between crown size and biomass. Nonetheless, the generation of maps of tropical forest crown size and heterogeneity using the FOTO method has the potential to reveal fundamental new insights into the macroecology of tropical forests, and may prove a useful tool for the monitoring of forest degradation and recovery.

ACKNOWLEDGEMENTS

This work has been funded by the Wiener-Anspach Fundation and the Fonds National pour la Recherche Scientifique (FNRS, Belgium). Part of the work was conducted during a 1-year visit by the lead author to the University of Oxford.

REFERENCES

Aragão, L.E.O.C., Malhi, Y., Metcalfe, D.B., *et al.* (2009) Above- and below-ground net primary productivity across ten amazonian forests on contrasting soils. *Biogeosciences Discussions*, **6**, 2441–2488.

Asner, G.P. & Warner, A.S. (2003) Canopy shadow in Ikonos satellite observations of tropical forests and savannas. *Remote Sensing of Environment*, **87**, 521–533.

Asner, G.P., Palace, M., Keller, M., Pereira, R., Silva, J.N.M. & Zweede, J.C. (2002) Estimating canopy structure in an Amazon Forest from laser range finder and Ikonos satellite observations. *Biotropica*, **34**, 483–492.

Aubréville, A. (1938) La forêt coloniale. les forêts de l'Afrique occidentale française. *Annales de l'Académie des Sciences Coloniales*, **9**, 1–245.

Baker, T.R., Phillips, O.L., Malhi, Y., Almeida, S., Arroyo, L., Di Fiore, A., Erwin, T., Higuchi, N., Killeen, T.J., Laurance, S.G., Laurance, W.F., Lewis, S.L., Monteagudo, A., Neill, D.A., Núñez Vargas, P., Pitman, N.C.A., Silva, J. N. M. & Vásquez Martínez, R. (2004) Increasing biomass in Amazonian forest plots. *Philosophical Transactions of the Royal Society B: Biological Sciences*, **359**, 353–365.

Bruniquel-Pinel, V. & Gastellu-Etchegorry, J.P. (1998) Sensitivity of texture of high resolution images of forest to biophysical and acquisition parameters. *Remote Sensing of Environment*, **65**, 61–85.

Couteron, P. (2002) Quantifying change in patterned semi-arid vegetation by Fourier analysis of digitized aerial photographs. *International Journal of Remote Sensing*, **23**, 3407–3425.

Couteron, P., Pélissier, R., Nicolini, E.A. & Paget, D. (2005) Predicting tropical forest stand structure parameters from Fourier transform of very high-resolution remotely sensed canopy images. *Journal of Applied Ecology*, **42**, 1121–1128.

Couteron, P., Barbier, N. & Gautier, D. (2006) Textural ordination based on Fourier spectral decomposition: a method to analyze and compare landscape patterns. *Landscape Ecology*, **21**, 555–567.

Cressie, N.A.C. (1993) *Statistics for spatial data*. Wiley, New York.

Defries, R., Achard, F., Brown, S., Herold, M., Murdiyarso, D., Schlamadinger, B. & de Souza, C. (2007) Earth observations for estimating greenhouse gas emissions from deforestation in developing countries. *Environmental Science and Policy*, **10**, 385–394.

Diggle, P. (1989) *Time series: a biostatistical introduction*. Oxford University Press, Oxford.

Ellenberg, H. (1975) Vegetationsstufen in perhumiden bis perariden Bereichen der tropischen Anden. *Phytocoenologia*, **2**, 368–387.

Enquist, B.J. (2002) Universal scaling in tree and vascular plant allometry: toward a general quantitative theory linking plant form and function from cells to ecosystems. *Tree Physiology*, **22**, 1045–1064.

Eva, H.D., Belward, A.S., De Miranda, E.E., Di Bella, C.M., Gond, V., Huber, O., Jones, S., Sgrenzaroli, M. & Fritz, S. (2004) A land cover map of South America. *Global Change Biology*, **10**, 731–744.

FAO, ISRIC, UNEP & CIP (1998) *Soil and terrain database for Latin America and the Caribbean (v2.0), 1:5M. scale* (CD-ROM). Land and Water Digital Media Series 5. FAO, Rome.

Foody, G.M. (2003) Remote sensing of tropical forest environments: towards the monitoring of environmental resources for sustainable development. *International Journal of Remote Sensing*, **24**, 4035–4046.

Frazer, G.W., Wulder, M.A. & Niemann, K.O. (2005) Simulation and quantification of the fine-scale spatial pattern and heterogeneity of forest canopy structure: a lacunarity-based method designed for analysis of continuous canopy heights. *Forest Ecology and Management*, **214**, 65–90.

Gastellu-Etchegorry, J.P., Demarez, V., Pinel, V. & Zagolski, F. (1996) Modeling radiative transfer in heterogeneous 3-D vegetation canopies. *Remote Sensing of Environment*, **58**, 131–156.

Huete, A., Didan, K., Miura, T., Rodriguez, E.P., Gao, X. & Ferreira, L.G. (2002) Overview of the radiometric and biophysical performance of the MODIS vegetation indices. *Remote Sensing of Environment*, **83**, 195–213.

Huete, A.R., Didan, K., Shimabukuro, Y.E., Ratana, P., Saleska, S.R., Hutyra, L.R., Yang, W.Z., Nemani, R.R. & Myneni, R. (2006) Amazon rainforests green-up with sunlight in dry season. *Geophysical Research Letters*, **33**, L06405, doi: 10.1029/2005GL025583

Longman, K.A. & Jenik, J. (1987) *Tropical forest and its environment*, 2nd edn. Longman Scientific and Technical, Harlow.

Malhi, Y. & Phillips, O. (2005) *Tropical forests and global atmospheric change*. Oxford University Press, Oxford.

Malhi, Y. & Roman-Cuesta, R.M. (2008) Analysis of lacunarity and scales of spatial homogeneity in Ikonos images of Amazonian tropical forest canopies. *Remote Sensing of Environment*, **112**, 2074–2087.

Malhi, Y. & Wright, J. (2004) Spatial patterns and recent trends in the climate of tropical rainforest regions. *Philosophical Transactions of the Royal Society B: Biological Sciences*, **359**, 311–329.

Malhi, Y., Phillips, O.L., Lloyd, J., *et al.* (2002) An international network to monitor the structure, composition and dynamics of Amazonian forests (RAINFOR). *Journal of Vegetation Science*, **13**, 439–450.

Malhi, Y., Baker, T.R., Phillips, O.L., *et al.* (2004) The above-ground coarse wood productivity of 104 Neotropical forest plots. *Global Change Biology*, **10**, 563–591.

Malhi, Y., Wood, D., Baker, T.R. *et al.* (2006) The regional variation of aboveground live biomass in old-growth Amazonian forests. *Global Change Biology*, **12**, 1107–1138.

Mougin, E., Proisy, C., Marty, G., Fromard, F., Puig, H., Betoulle, J.L. & Rudant, J.P. (1999) Multifrequency and multipolarization radar backscattering from mangrove forests. *IEEE Transactions on Geoscience and Remote Sensing*, **37**, 94–102.

Mugglestone, M.A. & Renshaw, E. (1998) Detection of geological lineations on aerial photographs using two-dimensional spectral analysis. *Computers and Geosciences*, **24**, 771–784.

Myneni, R.B., Yang, W.Z., Nemani, R.R. *et al.* (2007) Large seasonal swings in leaf area of Amazon rainforests. *Proceedings of the National Academy of Sciences USA*, **104**, 4820–4823.

Oldeman, R.A.A. (1990) *Forests: elements of silvology*. Springer-Verlag, Berlin.

Palace, M., Keller, M., Asner, G.P., Hagen, S. & Braswell, B. (2008) Amazon forest structure from Ikonos satellite data and the automated characterization of forest canopy properties. *Biotropica*, **40**, 141–150.

Phillips, O.L., Baker, T.R., Arroyo, L. *et al.* (2004) Pattern and process in Amazon tree turnover, 1976–2001. *Philosophical Transactions of the Royal Society B: Biological. Sciences*, **359**, 381–407.

Poorter, L., Bongers, L. & Bongers, F. (2006) Architecture of 54 moist-forest tree species: traits, trade-offs, and functional groups. *Ecology*, **87**, 1289–1301.

Proisy, C., Couteron, P. & Fromard, F. (2007) Predicting and mapping mangrove biomass from canopy grain analysis using Fourier-based textural ordination of Ikonos images. *Remote Sensing of Environment*, **109**, 379–392.

Richards, P.W. (1995) *The tropical rain forest: an ecological study*, 2nd edn. Cambridge University Press, Cambridge.

Saatchi, S.S., Houghton, R.A., Alvala, R.C.D.S., Soares, J.V. & Yu, Y. (2007) Distribution of aboveground live biomass in the Amazon basin. *Global Change Biology*, **13**, 816–837.

Saatchi, S., Malhi, Y., Zutta, B.R. *et al.* (2009) Mapping landscape scale variations of forest structure, biomass, and productivity in Amazonia. *Biogeosciences Discussions*, **6**, 5461–5505.

Saleska, S.R., Didan, K., Huete, A.R. & Da Rocha, H.R. (2007) Amazon forests green-up during 2005 drought. *Science*, **318**, 612.

van Schaik, C.P., Terborgh, J.W. & Wright, S.J. (1993) The phenology of tropical forests – adaptive significance and consequences for primary consumers. *Annual Review of Ecology and Systematics*, **24**, 353–377.

Sombroek, W. (2001) Spatial and temporal patterns of Amazon rainfall – consequences for the planning of agricultural occupation and the protection of primary forests. *Ambio*, **30**, 388–396.

ter Steege, H., Pitman, N.C.A., Phillips, O.L., Chave, J., Sabatier, D., Duque, A., Molino, J.F., Prévost, M.F., Spichiger, R., Castellanos, H., von Hildebrand, P. & Vásquez, R. (2006) Continental-scale patterns of canopy tree composition and function across Amazonia. *Nature*, **443**, 444–447.

Véga, C. & St-Onge, B. (2008) Height growth reconstruction of a boreal forest canopy over a period of 58 years using a combination of photogrammetric and lidar models. *Remote Sensing of Environment*, **112**, 1784–1794.

Watt, A.S. (1947) Pattern and process in the plant community. *Journal of Ecology*, **35**, 1–22.

Weishampel, J.F., Godin, J.R. & Henebry, G.M. (2001) Pantropical dynamics of 'intact' rain forest canopy texture. *Global Ecology and Biogeography*, **10**, 389–397.

Wolff, D.B., Marks, D.A., Amitai, E., Silberstein, D.S., Fisher, B.L., Tokay, A., Wang, J. & Pippitt, J.L. (2005) Ground validation for the tropical rainfall measuring mission (TRMM). *Journal of Atmospheric and Oceanic Technology*, **22**, 365–380.

Wright, S.J. (2005) Tropical forests in a changing environment. *Trends in Ecology and Evolution*, **20**, 553–560.

Wright, S.J. & van Schaik, C.P. (1994) Light and the phenology of tropical trees. *The American Naturalist*, **143**, 192–199.

SUPPORTING INFORMATION

Additional Supporting Information may be found in the online version of this article:

Figure S1 QuickBird canopy unit-windows dominated by specific ranges of spatial frequencies, and selected to illustrate the gradient of apparent crown size.

Figure S2 Selection of QuickBird unit-windows with several or no dominant spatial frequencies.

Figure S3 Standardized r-spectra for the representative unit-windows shown in Figs S1 & S2, and localized in the principal components analysis (PCA) plan.

Figure S4 More restrictive estimation of apparent crown size using a quadratic function (model inversion) of the two first components of the principal components analysis (PCA).

Table S1 List of QuickBird images, with values of acquisition parameters and results of textural ordination.

As a service to our authors and readers, this journal provides supporting information supplied by the authors. Such materials are peer-reviewed and may be re-organized for online delivery, but are not copy-edited or typeset. Technical support issues arising from supporting information (other than missing files) should be addressed to the authors.

BIOSKETCH

Nicolas Barbier is a post-doctoral FNRS fellow. The main focus of his research concerns the characterization, causality and dynamics of spatial structure in tropical vegetations.

Editor: José Paruelo